RESEARCH ARTICLE

Independent Molecular Development of Metachronous Glioblastomas with Extended Intervening Recurrence-free Interval

Ramon Martinez[1]; Hans-K. Schackert[2]; Stephanie von Kannen[1]; Peter Lichter[3]; Stefan Joos[3]; Gabriele Schackert[1]

[1] Departments of Neurosurgery and [2]Surgical Research of the University of Dresden, Germany.
[3] German Cancer Research Center (DKFZ),Heidelberg, Germany.

Two metachronous glioblastomas with different cerebral locations in a 53-year-old long-term survival patient were analyzed by multiple genetic approaches. Using comparative genomic hybridization a different pattern of chromosomal aberrations was observed, with 19 imbalances in the first tumor and only 2 imbalances in the second. Sequence analysis revealed a distinct mutation profile in each tumor, with amino acid substitutions in the *p53* and *PTEN* genes only in the first tumor, ie, *p53* in codon 273 (CGT→TGT, Arg→Cys) and *PTEN* in codon 336 (TAC→TTC, Tyr→Phe). A splicing acceptor site *PTEN* mutation (IVS8–2A>G) was observed only in the second GBM. *EGFR* amplification, mutations of *p16^{INK4a}/CDKN2A* or *p14^{ARF}* were not observed. According to the results of *p53* mutational analysis and *EGFR* amplification studies, the first tumor is classified as a type 1 GBM, whereas the alterations in the second one are different from those typically encountered in type 1 or type 2 tumors. In conclusion, our data strongly suggest that the metachronous tumors in this patient are exceptional in that they developed independently from each other. Whether the molecular features of the first glioblastoma are associated with the notably extended recurrence-free period of 5 years remains to be elucidated.

Brain Pathol 2003;13:598-607.

Introduction

Glioblastoma multiforme (GBM) is the most frequent intracranial tumor in adults and accounts for 12 to 15% of all brain neoplasms (18). Its prognosis is dismal with a median survival time of 12 months after diagnosis, despite aggressive therapy (20). Nevertheless, up to 2% of all GBM patients show a long-term survival of more than 3 years (29). The genetic factors, which are responsible for the long recurrence-free time are still unknown (4).

GBM may develop from a preexisting low-grade astrocytoma or arise de novo. Most of the de novo glioblastomas develop in the elderly and usually carry an amplification of the epidermal growth factor receptor (*EGFR*) oncogene. This situation has been termed type 2 glioblastomas (34). In contrast, type 1 glioblastomas tend to occur in younger patients and usually harbor a *p53* inactivation without an *EGFR* amplification (34, 15). About one third of GBMs show *EGFR* amplification and one third *p53* inactivation, while in about 30% of the cases other molecular alterations are observed (33, 22, 7).

GBMs have an inherent tendency to recur, most frequently locally. However, tumor cell migration through the cerebrospinal fluid (CSF) and midbrain are known to be implicated in distant relapses (28). Therefore, shared genetic alterations in GBMs and their recurrences could be anticipated (11). Nevertheless, metachronous GBMs with different brain localizations in the same patient might alternatively represent independent malignancies consequently harboring distinct molecular patterns. Both these concepts have raised controversial discussions, not only concerning the mechanistic point of view but also with regard to the development of rational therapeutic approaches (28).

Metachronous GBMs in a single patient represent a suitable model to investigate the multistep process of GBM carcinogenesis. In the present study, we investigated 2 metachronous glioblastomas, developing in different cerebral locations using multiple genetic and cytogenetic approaches. This included comparative genomic hybridization (CGH) for a comprehensive detection of chromosomal imbalances, LOH analysis, mutational screening of *p53*, *PTEN*, *p16^{INK4a}/CDKN2A* and *p14^{ARF}*, immunohistochemical studies as well as assessment of the mismatch repair (MMR) system. Since the patient studied had a long recurrence-free time lapse after the treatment of the first tumor (5 years) but not after the second one (1.5 years), the present analysis should

Corresponding author:
R. Martinez, MD. Department of Neurosurgery, Klinikum Fulda, Academic Hospital Philipps-University Marburg, Pacelliallee 4, D-36043 Fulda, Germany (E-mail: voelter.martinez@t-online.de)

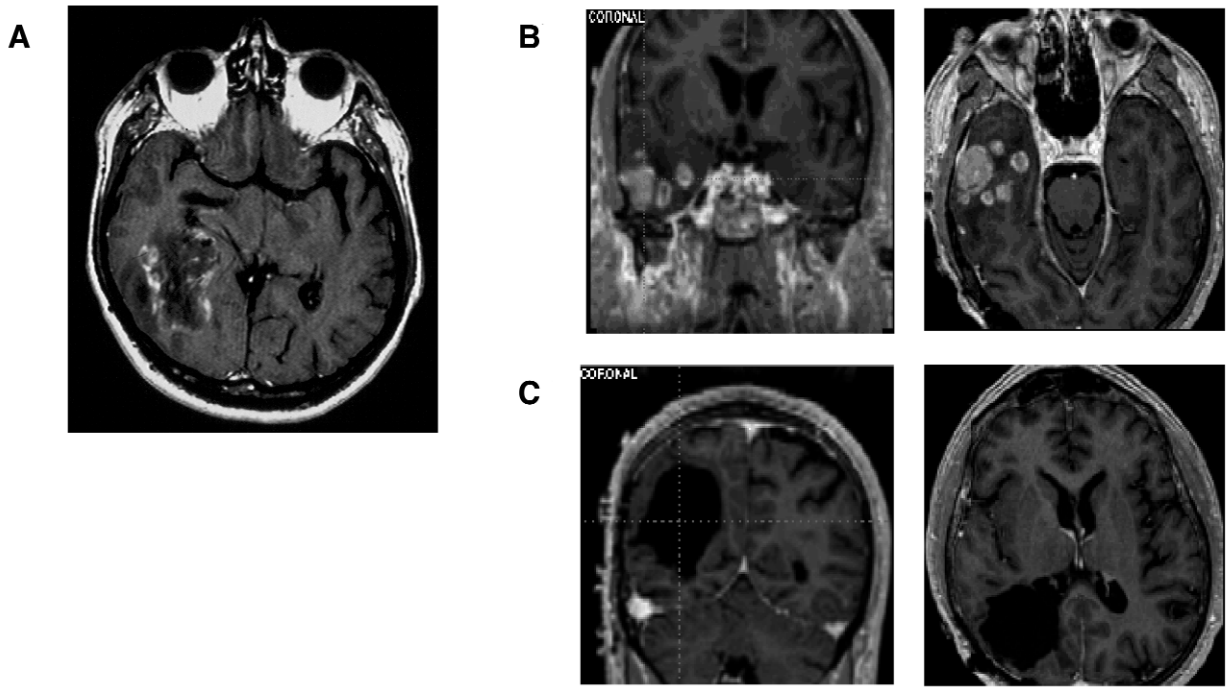

Figure 1. A. T1-weighted MRI examinations of the first tumor. A gadolinium-enhanced lesion in the right parieto-occipital lobes with necrosis areas and edema is shown. **B, C.** Gadolinium enhanced T1-weighted MRI scans of the second GBM (**B**) showing a right temporal tumor 5 years after the resection of the first GBM (**C**). A local re-growth of the first tumor was not found.

also contribute to the understanding of the genetic factors associated with long-term survival in GBMs.

Material and Methods

Clinical findings. The 53-year-old patient was initially admitted in our Neurosurgical Department with complaints of loss of concentration, irritability and memory impairment. He had no family or personal history of cancer. The clinical examination showed a left homonymous hemianopsia and motor skills detriment. A MRI scan revealed a gadolinium enhanced mass lesion involving the right parieto-occipital lobes (Figure 1A). The patient underwent a right osteoplastic craniotomy with complete tumor resection. Local fractionated radiotherapy and chemotherapy with ACNU and VM 26 (teniposide) were also postoperatively carried out. After an unusually long recurrence-free time span of five years, the patient developed a new tumor involving the basal right temporal lobe, which grew rapidly as demonstrated by two consecutive MRIs (Figure 1B, C). A right fronto temporal craniotomy was subsequently performed and the second tumor was completely resected. The patient underwent postoperative fractionated radiotherapy and chemotherapy with temozolomide. Eighteen months after resection of the second GBM he developed multiple tumors in the midbrain. The patient died 6.5 years after the first surgical procedure.

Methods. Intraoperatively, tissue from different tumor areas was resected for research purposes, avoiding tumor margins. Fresh tumor samples were frozen immediately in liquid nitrogen after removal and stored at -80°C. Formalin-fixed, paraffin-embedded materials were used for immunohistochemical analysis. Representative and abundant tumor tissue samples were evaluated by experienced pathologists of the Institute of Pathology, University of Dresden, Germany and independently reviewed at the Institute of Neuropathology according to the World Health Organization (WHO) criteria at the German Brain Tumor Reference Center (University Bonn, Germany). Peripheral blood samples, which were used as a source of constitutional DNA, were obtained at the time of tumor resections.

Comparative genomic hybridization. Metaphase chromosomes were prepared from healthy female individuals according to standard protocols. Probe preparation, hybridization, and image acquisition were performed as described previously (16, 17). Gray level

images of 10 to 15 metaphase cells were recorded separately for each fluorochrome and the ratio of FITC:TRITC fluorescence intensities along each individual chromosome was calculated and averaged (9) using dedicated software (CytoVision 3.52, Applied Imaging International Ltd. Sunderland, United Kingdom). Chromosomal imbalances were detected on the basis of the ratio profile deviating from the balanced value 1.0 with the values 1.25 and 0.75 as diagnostic cutoff levels for over- and underrepresentations of chromosomal material, respectively.

LOH analysis. In order to ensure patient-tumor identity we studied the polymorphic markers D3S1358, D13S317, D5S818, CSF1PO, D7S820, D21S11 and TH01 in DNA from both tumor samples and patient blood leukocytes. PCR reactions were carried out using 50 ng of template DNA, with an initial denaturation temperature of 94°C and a final extension of 72°C. Primer sequences and PCR amplification conditions are based on Genome Database entries (*http://www.gdb.org*).

LOH of chromosome 10q was studied with markers covering reported deletions on 10q23-24: D10S215 and D10S541 (both flanking the locus *PTEN*, ≤1 cM), the *PTEN* intragenic marker PTENCA, D10S583 and D10S579 (telomeric and centromeric to *PTEN*, respectively), spanning a distance of 10 cM of the *PTEN* locus (13). Analysis of LOH at 17p13 was performed with TP53 and a *p53* intragenetically localized marker (primer sequences available from the authors).

Allelic losses at 9p21 (*$p16^{INK4a}$/CDKN2A*, *$p14^{ARF}$* and *p15/CDKN2B* loci) and 13q14 (*RB1*) were studied with primers D9S171, D9S1748, D9S1749, D13S153 and D13S267. Loss of heterozygosity at 1p35-p36 and 19q13 was assessed with the markers D1S468, D1S482, D19S112 and D19S412 as previously described (19, 30).

Amplified PCR products were analyzed on a denaturing 6.5% Long Ranger polyacrylamide gel on an Automated Laser Fluorescence (A.L.F. express®) sequencing device (Amersham Pharmacia Biotech, Freiburg, Germany) and analyzed using the ALLELELINKS® 1.00 software (Amersham Pharmacia Biotech). Evaluation of LOH was performed using a semiquantitative method as described (5). LOH studies for all analyzed markers were performed using the same DNA pool.

Semiquantitative PCR-analysis. To test for *PTEN* homozygous deletions, we established a comparative differential PCR consisting of one standard primer pair outside the region of suspected deletion (*CFTR*) and a primer pair that was intragenetically localized (PTENCA). To determine the standard ratio between the test and standard marker, leukocyte DNA samples from ten healthy Caucasian individuals were co-amplified in each multiplex PCR. Peak reductions in PTENCA were scored as homozygous deletion if the ratio PTENCA/CFTR was less than the value [(x-3SD)/2] (10).

For studying amplification of *EGFR* a differential duplex-PCR with the *CFTR*-(cystic fibrosis transmembrane regulator) gene marker was carried out (27). Briefly, we calculated the *EGFR*/*CFTR* ratios (x) from peripheral blood DNA of 30 healthy Caucasian adults. A value (x+3SD) was considered as the cut-off level for the normal gene copy number. Ratios higher than (x+3SD) were regarded as evidence of more than 2 copies of the *EGFR* gene.

Sequencing analysis of p53, PTEN, $p16^{INK4a}$ and $p14^{ARF}$. Mutational analysis of *p53* (exons 2-11), *PTEN* (exons 1-9), *$p16^{INK4a}$/CDKN2A*, (exons 1a and 2) and *$p14^{ARF}$* (exons 1b and 2) were performed in the DNA from both tumors and leukocytes. After amplifying all exons and intron-exon boundaries, we analyzed the PCR products on 1% agarose gel and excised and eluted them in sterile H_2O. Subsequently, they were subjected to cycle sequencing reactions using the Thermo Sequenase® Fluorescent Cycle Sequencing kit (Amersham Pharmacia Biotech). The cycle sequencing products were resolved using a denaturing 6.5% Long Ranger polyacrylamide gel on an sequencing device. *PTEN* primer sequences and PCR conditions were previously described (21, 31). Primer sequences and amplification conditions for *$p16^{INK4a}$*, *$p14^{ARF}$* and *p53* are available from the authors.

Analysis of microsatellite instability (MSI). MSI evaluation was performed using 15 microsatellite markers distributed over 9 different chromosomes (8): mononucleotide repeats (BAT25, BAT26, BAT40, TGFβ-RIIpA, GTBPIn5, GTBPIn9), dinucleotide repeats (D5S346, D17S250, D10S197, D2S123, D18S58, D13S153, D3S1300, D3S1619) and tetranucleotide repeat (MYCL1). PCR products were visualized using a denaturing 6.5% Long Ranger polyacrylamide gel on an A.L.F. express® sequencing device and analyzed using the software ALLELELINKS® 1.00. MSI was defined by the presence of novel peaks in tumor DNA, which were absent in corresponding leukocyte DNA.

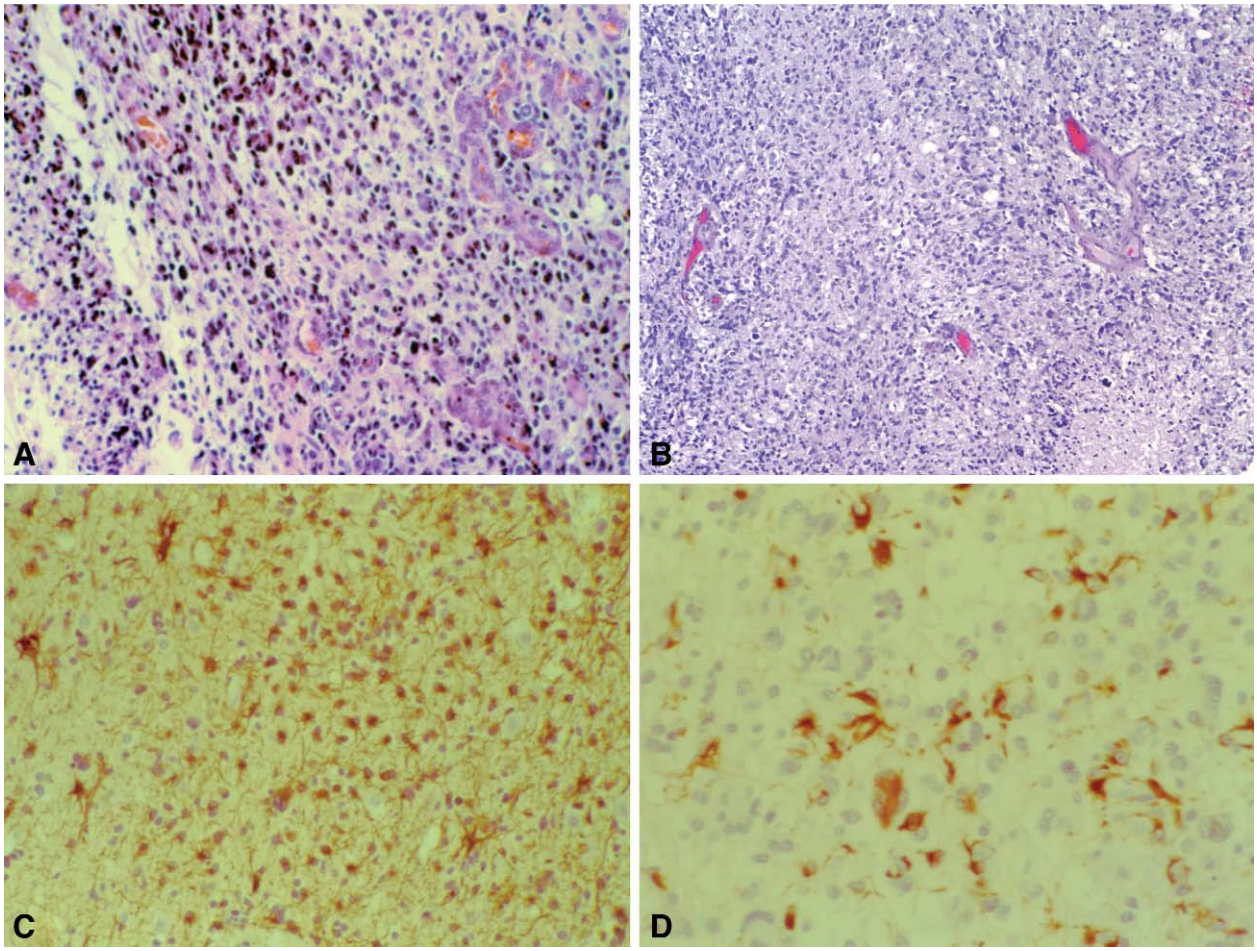

Figure 2. Photomicrographs showing staining of fractions of tumor cells for H&E (hematoxylin-eosin) in the upper row and GFAP (glial fibrillary acidic protein) in the lower row. Microvascular proliferation, pseudopalisading and necrosis is evidenced in the first GBM (**A**, **C**). The second GBM shows mitoses in lower pics and necrosis as well (**B**, **D**). Original magnifications are x 100, x 200 (H&E) and ×200, ×400 (GFAP).

Immunohistochemistry. Immunostaining for the mismatch repair gene products *MSH2* (clone FE11, Oncogene Res. Products, Cambridge, Mass), *MLH1* (clone G168-15, PharMingen Int., San Diego, Calif), *MSH6* (clone 44, Transduction Lab., Lexington, Ky) and *PMS2* (A16-4, PharMingen Int., San Diego, Calif) was performed as previously described (25). The normal staining pattern for the antibodies was nuclear. The relative densitometry of MMR protein expression was performed using the Meta-Vue® software (Universal Imaging Systems, Pa). Furthermore, we used primary antibodies against the proliferation-associated nuclear antigen Ki67 (monoclonal mouse anti-human, Novocastra Laboratories Ltd., Newcastle, United Kingdom), the glial fibrillary acidic protein GFAP (monoclonal mouse anti-human, Dako A/S, Glostrup, Denmark), vimentin and cytokeratin (V9 and Lu-5, respectively; both from Roche Molecular Biochemicals, Mannheim, Germany), p16 (monoclonal mouse anti-human, Santa Cruz Biotechnology, Santa Cruz, Calif), p18 (monoclonal mouse anti-human, Santa Cruz Biotechnology, Santa Cruz, Calif) and p53 (monoclonal mouse anti-human, Biogenex, San Ramon, Calif). For negative controls, sections were processed as described above without adding the primary antibodies.

Results

Histopathological and immunohistochemical analysis. Concerning the first tumor a highly cellular tumor of glial origin was observed (Figure 2). Gemistocytic tumor cells demonstrated mitosis. Pleomorphic cells containing atypical nuclei with numerous atypical

Immunohistochemical study	First glioblastoma	Second glioblastoma
p53	Positive (100%)	Positive (80%)
Glial fibrillary acidic protein (GFAP)	Positive	Positive
Proliferation associated nuclear antigene Ki67 (MIB-1)	Positive (5-10%)	Positive (30%)
S-100 protein	Positive	Negative
Vimentin (V9)	n.d.	Negative
Cytokeratin (Lu-5)	Negative	Negative
p16	Positive	Negative
p18	Positive	Positive

n.d. = not done

Table 1. Summary of immunohistochemical findings in both GBMs.

mitotic figures were observed as well. The lesion demonstrated areas of pseudopalisading necrosis and microvascular proliferation. Additionally, necrotic vessels and large necrotic tumor foci were found. In large areas of the specimen, a network of reticulin fibers was present between tumor cells. Oligodendroglial-like tumor cells with round nuclei and honeycomb appearance were rarely found. The histological analysis of the second specimen revealed a highly cellular astrocytic tumor with areas of necrosis, microvascular proliferation, necrotic vessels and more mitotic figures than in the first GBM. Areas suggestive of a less malignant astrocytic tumor were not observed in any of the specimen. Pleomorphic giant tumor cells containing multiple nuclei were only occasionally observed in both tumors.

In the second specimen, immunohistochemical studies showed a higher proliferation activity as demonstrated by the nuclear antigen MIB-1 labeling index (Table 1). In contrast to the first GBM, which showed a strong GFAP staining, the expression of GFAP was recognizable in fewer fractions of tumor cells (Figure 2). Nuclear accumulation of p53 protein was shown in a significant fraction of tumor cells, more widely in the first sample. Based on these findings the diagnosis of glioblastoma multiforme (World Health Organization grade IV) was established in both cases.

Comparative genomic hybridization. Comparative genomic hybridization (CGH) of the first tumor showed gains of chromosomal bands 2q22-q33, 3p11-p13, 3q11-q13, 3q26, 4p, 4q11-q12, 5q14-q23, 6p11-p12, 6q11-q22, 7q31, 8q13-qter, 11q13-qter, 12p13, 12q21, 13q21-q31 and losses at 8p23, 10q23-26, 11p15, and 14q24-q31. In the second tumor gains of 3p22-p24 and of 8q24 were detected. Chromosomal region 8q24 is therefore overrepresented in the first and the second tumor (Figure 3).

LOH analysis of p53, PTEN, p16^{INK4a} and p14^{ARF}. Microsatellite analysis of tumor sample identity using highly polymorphic markers revealed an identical pattern in all markers tested.

LOH at 17p13 was found only in the first GBM, whereas the second one showed no allelic loss. LOH on chromosome 10q was present in both tumor specimens. The first GBM showed LOH at both markers flanking the *PTEN* locus (D10S541 and D10S215) as well as for the intragenetic PTENCA marker. In the second GBM, the allelic balance at the former markers was maintained but there was an allelic loss at D10S583, telomeric to the *PTEN* locus.

A region of hemizygous deletion at 9p21 in the first GBM included the locus D9S1748, centromeric of *CDKN2A* and telomeric of *CDKN2B*. No allelic losses were observed at the loci D9S171 and D9S1749 (centromeric and telomeric of *CDKN2A* and *CDKN2B*, respectively). There were no losses at 9p21 in the second tumor.

A region of allelic deletion at chromosome 19q was identified between 19q13.2-19q13.4 in the first resected GBM (allelic losses at D19S112 and the telomeric locus D19S412). The second GBM showed retention of heterozygosity at the corresponding site. Both tumors maintained allelic balance at 1p35-p36.

Semiquantitative PCR of PTEN and EGFR. Homozygous deletions of *PTEN* were not observed in any

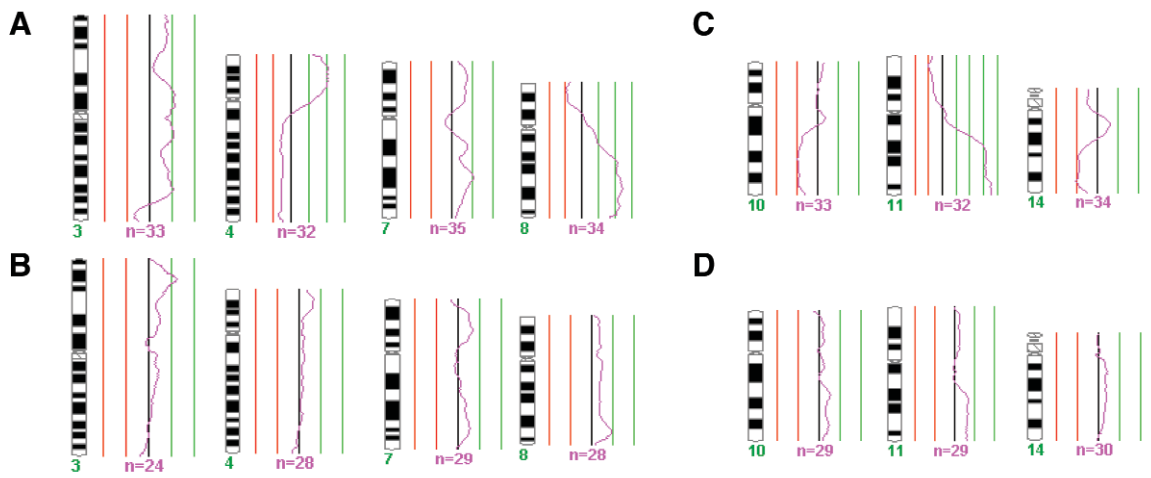

Figure 3. CGH results of selected chromosomes from the first (upper rows: **A**, **C**) and second GBM (lower rows: **B**, **D**) showing gains and losses of chromosomal regions. The central line indicates the balanced state of chromosomal material within the tumor genome. The right and left lines represent cut-off values for chromosomal gains and losses, respectively (ie, 1.25 and 0.75).

tumor. The PTENCA/ CFTR ratio of the control DNA specimens was 0.262. The ratios in the first and second GBM were 0.52 and 0.47, respectively. With respect to *EGFR*, the *EGFR/CFTR* ratios were 1.47 and 0.53 for the first and second GBM, respectively, being less than the value (x+3SD). This indicated the absence of *EGFR* amplification in any of the tumors.

Mutational analysis of p53, PTEN, p16^{INK4a} and p14^{ARF}. In the first GBM a single base pair exchange in the *p53* gene was identified (codon 273, CGT→TGT) predicting the substitution of arginine (Arg^{273}) by cysteine (Cys^{273}) (Figure 4A, B), which was found to be associated with a complete loss of the wild-type allele. We did not find this *p53* mutation in the DNA from the second GBM. No germline alterations were observed by sequencing *p53* from leukocyte DNA.

The sequence analysis of *PTEN* (Figure 4C-E) revealed the following mutations in the first but not in the second GBM on exon 8, codon 335 (CGA→CGT, Arg→Arg) and codon 336 (TAC→TTC, Tyr→Phe) as well as the intronic hemizygous mutations IVS8+23 T>G and IVS8+16 C>A. Furthermore, a splicing acceptor site mutation was found only in the second GBM, IVS8–2 A>G. Two polymorphisms were detected, on exon 8 (codon 338 TCT→TCC, Ser→Ser) and 32 nucleotides downstream of exon 8 (IVS8+32 G>T).

Sequencing of exons 1a and 2 of *p16^{INK4a}* and 1b and 2 of *p14^{ARF}* revealed no alterations in either GBM.

Analysis of the mismatch repair system. No instability was observed using the 15 polymorphic markers described above, indicating a microsatellite stable phenotype (MSS). In addition, immunohistochemical analysis of the DNA mismatch repair gene products *MLH1*, *MSH2*, *MSH6* and *PMS2* showed a positive nuclear staining. Densitometric analysis of the expression of all MMR proteins was performed in 50 tumor cells from each tumor. There was no significant difference in the immunoreactivity of the proteins analyzed in either glioblastomas (t-test: P>0.05).

Discussion

GBMs are clonal tumors (23) with an inherent tendency to recur. Shared genetic alterations in GBMs and their recurrences are expected and have been previously reported (11, 28). Nevertheless, metachronous GBMs in individual patients might alternatively represent multiple malignancies harboring distinct molecular patterns. To our knowledge, there is only one molecular study indicating the independent development of a second de novo GBM (26).

Several remarkable clinical aspects render the patient investigated unique and already pointed at an independent development of both tumors: first, the tumors were clinically de novo GBMs without histopathological signs of less malignant precursor areas; second, the different brain locations of both lesions; and third, the unusual relapse-free interval of 5 years of the first tumor but 1.5 years of the second with only the latter time

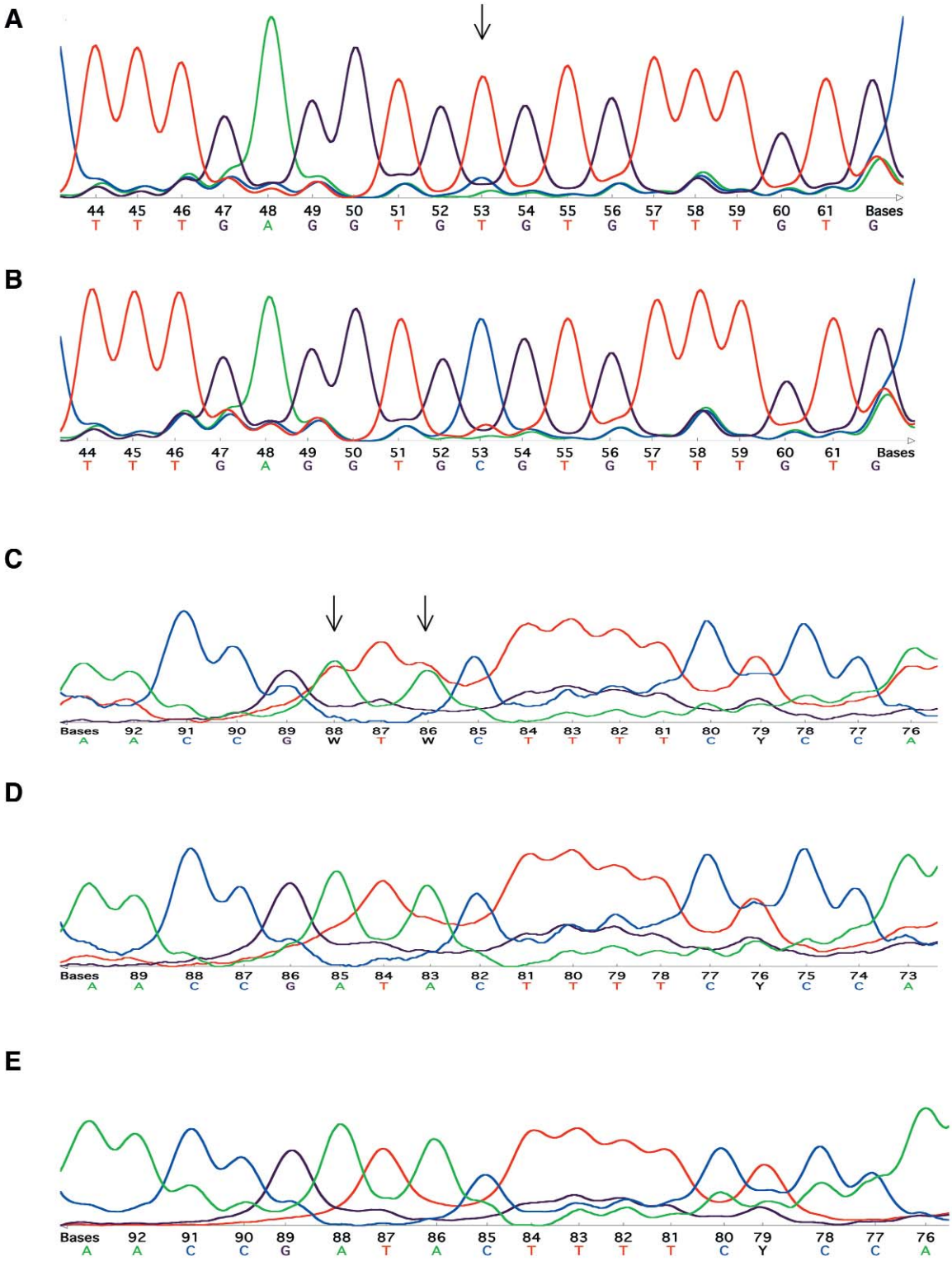
A
44 45 46 47 48 49 50 51 52 53 54 55 56 57 58 59 60 61 Bases
T T T G A G G T G T G T G T T T G T G
B
44 45 46 47 48 49 50 51 52 53 54 55 56 57 58 59 60 61 Bases
T T T G A G G T G C G T G T T T G T G
C
Bases 92 91 90 89 88 87 86 85 84 83 82 81 80 79 78 77 76
A A C C G W T W C T T T T C Y C C A
D
Bases 89 88 87 86 85 84 83 82 81 80 79 78 77 76 75 74 73
A A C C G A T A C T T T T C Y C C A
E
Bases 92 91 90 89 88 87 86 85 84 83 82 81 80 79 78 77 76
A A C C G A T A C T T T T C Y C C A

being within the expected range in the progression of GBMs.

To address the underlying genetic mechanisms, we initially performed a CGH analysis. In general, the pattern of genomic imbalances of each specimen was different in that multiple aberrations were detected only in the first GBM. The paucity of genomic alterations observed in the second tumor is unusual in GBMs (1) and may point to a different pathogenetic mechanism. Overrepresentation of chromosomal band 8q24 was the only common cytogenetic finding suggesting that the *MYC* oncogene was involved in the pathogenesis of both tumors. Notably, no gain of chromosomal band 7p12 indicative of an amplification of the *EGFR* oncogene was detected.

In order to test whether the small number of chromosomal imbalances in the second GBM was associated with a deficient MMR, we analyzed MSI (2) and performed an immunohistochemical analysis of the MMR gene products. Since we found neither MSI nor loss of expression of the MMR proteins the paucity of chromosomal alterations is not likely to be related with inactivation of major MMR genes.

The LOH analysis also revealed significant differences in both GBMs. Specifically the LOH of *p53*, $p16^{INK4a}$, $p14^{ARF}$ and microsatellite locus on chromosomal arm 19q, were exclusively detected in the first tumor, while only *PTEN* showed LOH in both cases. The absence of 1p loss in both specimens and 19q in the second one remarked the lack of a substantial oligodendroglial component.

An independent development of both glioblastomas was further indicated by the distinct mutation patterns of *p53* and *PTEN*. The sequencing of *p53* identified alterations only in the first GBM, which harbored a single base pair exchange (codon 273). The residue Arg^{273} is one of the principal mutation targets within the *p53* gene, also in brain tumors (24). Arg^{273} directly contacts the DNA and is critical in stabilizing the p53 protein-DNA interface (6). Since *p53* mutations are early events in astrocytoma progression, it is unlikely that they had been lost in the present case. Concerning *PTEN*, 2 hemizygous mutations in the first GBM (codons 335 and 336) are of relevant interest. The Arg^{335} residue is a mutational hot spots of *PTEN*. Six germline *PTEN* mutations (in patients with Cowden disease and Bannayan-Riley-Ruvalcaba-syndrome) as well as 5 somatic mutations were reported in this residue in patients with GBM and endometrial carcinoma (3). Mutations at Tyr^{336} were previously described as well (3). In contrast to our findings, most of the previously reported *PTEN* mutations were localized in exon 6 (27%) whereas only few in exon 8 (12.7%) and exon 7 (8%) (3).

Strikingly, the same mutational mechanism was observed at Arg^{273} of *p53* gene and Arg^{335} of *PTEN* in the first GBM. Both mutations were C:G→A:T transitions at CpG islands (28) and they are considered to be caused endogenously as a consequence of the spontaneous deamination of 5-methylcytosine residues. This deamination process results in thymine leading to C-T transitions (sense strand) or G-A transitions (antisense strand) and it is normally corrected by a base excision repair mechanism as previously observed in different human cell types (14). The same observation was found in glioblastomas in a previous study (26), which might suggest a deficient base excision repair system.

Based on our data of *p53* mutational analysis and *EGFR* amplification both tumors investigated are exceptional, since they developed clinically de novo but genetically the first one showed a type 1 profile; whereas the second one was ascribed to the group of GBMs, which correspond neither to type 1 nor to type 2 (7).

Since radiotherapy was performed after the first surgical procedure, the possibility that the second GBM arose as a consequence of a rare radiation-induced hit has to be considered. However, we did not find alterations such as base pair deletions in *p53* or *PTEN* in the second tumor, which would be indicative for radiation induced DNA damage (32).

In summary, we have demonstrated distinct genetic and cytogenetic patterns in the studied metachronous glioblastomas. The mutational profile of the first tumor (a type 1 GBM) hints to a mechanism characterized by a deficient repair of deamination of 5-methylcytosyne residues and it concurred clinically with a extended recurrence-free interval of 5 years. A larger number of cases will be required to further examine the relevance of the described molecular alterations to prognosis of patients with GBM. The second glioblastoma (a non-type 1, non-type 2 GBM) showed a notable paucity in both chromosomal aberrations and alterations of those genes

Figure 4. (Opposing page) **A, B.** A *p53* single base pair exchange in codon 273 (CGT→TGT) in the first GBM predicts the substitution Arg→Cys (**A**). The second tumor (**B**) did not show this mutation. **C-E.** Sequencing of *PTEN* in the first glioblastoma evidenced 2 hemizygous mutations in exon 8, in codons 335 (CGA→CGT) and 336 (TAC→TTC). **C**, **D** and **E** represent sequences of first GBM, second GBM and leukocytes, respectively.

frequently implicated in GBM pathogenesis. Our analyses of both GBMs provide evidence for different underlying mechanisms of tumor genesis.

Acknowledgments

The authors thank the Institute of Neuropathology, German Brain Tumor Reference Center (Chairman Prof Dr O.D. Wiestler), University of Bonn for neuropathological re-evaluation of tumor samples. We also thank Prof Dr W. Paulus, Chairman of the Department of Neuropathology, University of Münster, Germany, Dr C. Voelter, ENT Department, University of Würzburg and K. Mueller, PhD, for helpful discussion and Mrs M. Reichmann, Department of Surgical Research, University of Dresden for skillful technical assistance.

Supported by a grant from the Deutsche Forschungsgemeinschaft, DFG (MA 2448/1) and the National Genome Research Network, Germany (KB-P6T06).

References

1. Bigner SH, Schröck E (1997) Molecular cytogenetics of brain tumors. *J Neuropathol Exp Neurol* 56:1173-1181.
2. Boland R, Thibodeau S, Hamilton S, Sidransky D, Eshleman J, Rodriguez-Bigas M, Fodde R, Ranzani GN, Srivastava S (1998) A National Cancer Institute workshop on microsatellite instability for cancer detection and familial predisposition: development of international criteria for the determination for microsatellite instability in colorectal cancer. *Cancer Res* 58:5248-5257.
3. Bonneau D, Longy M (2000) Mutations of the human PTEN gene.*Human Mutat* 16:109-122.
4. Burton EC, Lamborn KR, Forsyth P, Scott J, O´Campo J, Uyehara-Lock J, Prados M, Berger M, Passe S, Uhm J, O´Neill B, Jenkins RB, Aldape KD (2002) Aberrant p53, mdm2 and proliferation differ in glioblastomas from long-term compared with typical survivors. *Clin Cancer Res* 8:180-187.
5. Cawkwell L, Lewis FA, Quirke P (1994) Frequency of allele loss of DCC, p53, RB1, WT1, NF1, NM23 and APC/MCC in colorectal cancer assayed by fluorescent multiplex polymerase chain reaction. *Br J Cancer* 70:813-818.
6. Cho Y, Gorina S, Jeffrey P Pavletich NP (1994) Crystal structure of a p53 tumor suppressor DNA complex: a framework for understanding how mutations inactivate p53. *Science* 265:346-355.
7. Collins VP (1998) Gliomas. *Cancer Survey* 32:37-51.
8. Dietmaier W, Wallinger S, Bocker T, Kullman F, Fishel R and Ruschoff J (1997) Diagnostic microsatellite instability: definition and correlation with mismatch repair protein expression. *Cancer Res* 57:4749-4756.
9. Du Manoir S, Schröck E, Bentz M, Speicher MR, Joos S, Ried T, Lichter P, Cremer T (1995) Quantitative analysis of comparative genomic hybridization. *Cytometry* 19:27-41.
10. Duerr EM, Rollbrocker B, Hayashi Y, Peters N, Meyer-Puttlitz B, Louis DN, Schramm J, Wiestler OD, Parsons R, Eng C, von Deimling A (1998) PTEN mutations in gliomas and glioneuronal tumors. *Oncogene* 16:2259-2264.
11. Fujisawa H, Kurrer M, Reis RM, Yonekawa Y, Kleihues P, Ohgaki H (1999) Acquisition of the glioblastoma phenotype during astrocytoma progression is associated with loss of heterozygosity on 10q25-qter. *Am J Pathol* 155:387-394.
12. Greenblatt MS, Bennett M, Hollstein M, Harris CC (1994) Mutations in the p53 tumor suppressor gene: clues to cancer etiology and molecular pathogenesis. *Cancer Res* 54:4855-4878.
13. Hahn M, Wieland I, Koufaki ON, Görgens H, Sobottka SB, Schackert G, Schackert HK (1999) Genetic alterations of the tumor suppressor gene PTEN/MMAC1 in human brain metastases. *Clin Cancer Res* 5:2431-2437.
14. Hainaut P, Soussi T, Shomer B, Hollstein M, Greenblatt M, Hovig E, Harris CC, Montesano R (1997) Database of p53 gene somatic mutations in human tumors and cell lines: updated compilation and future prospects. *Nucleic Acids Res* 25:151-157.
15. Hayashi Y, Ueki K, Waha A, Wiestler OD, Louis DN, von Deimling A (1997) Association of gene amplification and CDKN2A (p16/MTS1) gene deletion in glioblastoma multiforme. *Brain Pathol* 7:871-875.
16. Joos S, Bergerheim USR, Pan Y, Matsuyama H, Bentz M, du Manoir S, Lichter P (1995) Mapping of chromosomal gains and losses in prostate cancer by comparative genomic hybridization. *Genes Chromosomes Cancer* 14:267-276.
17. Joos S, Otaño-Joos MI, Ziegler S, Brüderlein S, du Manoir S, Bentz M, Möller P, Lichter P (1996) Primary mediastinal (thymic) B-cell lymphoma is characterized by gains of chromosomal material including 9p and amplification of the REL gene. *Blood* 87:1571-1578.
18. Kleihues P, Ohgaki H (1999) Primary and secondary glioblastomas: from concept to clinical diagnosis. *Neurooncol* 1:44-51.
19. Kraus JA, Lamszus K, Glesmann N, Beck M, Wolter M, Sabel M, Krex D, Klockgether T, Reifenberger G, Schlegel U (2001) Molecular genetic alterations in glioblastomas with oligodendroglial component. *Acta Neuropathol* 101:311-320.
20. Lacroix M, Abi-Said D, Fourney DR, Gokaslan ZL, Shi W, DeMonte F, Lang FF, McCutcheon IE, Hassenbusch SJ, Holland E, Hess K, Michael C, Miller D, Sawaya R (2001) A multivariate analysis of 416 patients with glioblastoma multiforme: prognosis, extent of resection and survival. *J Neurosurg* 95:190-198.
21. Liaw D, Marsh DJ, Li J, Dahia PL, Wang SI, Zheng Z, Bose S, Call KM, Tsou HC, Peacocke M, Eng C, Parsons R (1997) Germline mutations of the PTEN gene in Cowden disease, an inherited breast and thyroid cancer syndrome. *Nat Genet* 16:64-67.
22. Louis DN (1997) A molecular genetic model of astrocytoma histopathology. *Brain Pathol* 7:755-764.
23. Morse RP, Darras BT, Ye Z, Wu JK (1994) Clonal analysis of human astrocytomas. *J Neurooncol* 21:151-157.

24. Nigro JM, Baker SJ, Preisinger AC, Jessup JM, Hostetter R, Cleary K, Bigner SH, Davidson N, Baylin S, Devilee P, Glover T, Collins FS, Weston A, Modali R, Harris CC, Vogelstein B (1989) Mutations in the p53 gene occur in diverse human tumor types. *Nature* 342:705-708.
25. Plaschke J, Kruger S, Pistorius S, Theissig F, Saeger HD, Schackert HK (2002) Involvement of hMSH6 in the development of hereditary and sporadic colorectal cancer revealed by immunostaining is based on germline mutations, but rarely on somatic inactivation. *Int J Cancer* 97:643-648.
26. Reis RM, Herva R, Brandner S, Koivukangas J, Mironov N, Bär W, Kleihues P, Ohgaki H (2001) Second primary glioblastoma. *J Neuropathol Exp Neurol* 60:208-215.
27. Rollbrocker B, Waha A, Louis DN, Wiestler OD, von Deimling A (1996) Amplification of the cyclin dependent kinase 4 (CDK4) gene is associated with high cdk4 protein levels in glioblastoma multiforme. *Acta Neuropathol* 92:70-74.
28. Saxena A, Shriml L, Dean M, Ali IU (1999) Comparative molecular genetic profiles of anaplastic astrocytomas/glioblastomas multiforme and their subsequent recurrences. *Oncogene* 18:1385-1390.
29. Scott JN, Rewcastle NB, Brasher PMA, Fulton D, Hagen NA, MacKinnon JA, Hamilton M, Cairncross JC, Forsyth P (1999) Which glioblastoma multiforme patient will become a long-term survivor? A population based study. *Ann Neurol* 46:183-188.
30. Smith JS, Perry A, Borell TJ, Lee HK, O'Fallon J, Hosek SM, Kimmel D, Yates A, Burger PC, Scheithauer BW, Jenkins RB (2000) Alterations of chromosome arms 1p and 19q as predictors of survival in oligodendrogliomas, astrocytomas, and mixed oligoastrocytomas. *J Clin Oncol* 18:636-645.
31. Steck PA, Pershouse MA, Jasser SA, Yung WK, Lin H, Ligon AH, Langford LA, Baumgard ML, Hattier T, Davis T, Frye C, Hu R, Swedlund B, Teng DH, Tavtigian SV (1997) Identification of a candidate tumor suppressor gene, MMAC1, at chromosome 10q23.3 that is mutated in multiple advances cancers. *Nat Genet* 15:356-362.
32. Tada M, Sawamura Y, Abe H, Iggo R (1997) Homozygous p53 gene mutation in a radiation-induced glioblastoma 10 years after treatment for an intracranial germ-cell tumor: case report. *Neurosurgery* 40:393-396.
33. Von Deimling A, Louis DN, Wiestler OD (1995) Molecular pathways in the formation of gliomas. *Glia* 15:328-338.
34. Von Deimling A, von Ammon K, Schoenfeld D, Wiestler OD, Seizinger BR, Louis DN (1993) Subsets of glioblastoma multiforme defined by molecular genetic analysis. *Brain Pathol* 3:19-26.